Available online at www.sciencedirect.com

SCIENCE DIRECT®

Journal of Molecular Catalysis A: Chemical 200 (2003) 301–313

JOURNAL OF MOLECULAR CATALYSIS A: CHEMICAL

www.elsevier.com/locate/molcata

Catalytic properties of Fe ion-exchanged mordenite toward the ethanol transformation: influence of the methods of preparation

Mohamed Mokhtar Mohamed

Department of Chemistry, Faculty of Science, Benha University, Benha, Egypt

Received 11 June 2002; accepted 14 January 2003

Abstract

The transformation of ethanol on Fe ion-exchanged mordenite was compared in the temperature range of 200–400 °C for samples prepared in the solution and solid states. Ethane and methane were found as rather major products, compared to acetaldehyde and acetone. Diethyl ether was also detected as a dehydration product. The conversion was found to increase monotonically (to 96%) with increasing the Fe content (to 100%) and reaction temperature to 400 °C. The selectivity towards acetaldehyde and acetone was found maximum at the temperature 300 °C. Decrease in the catalyst Brönsted acidity due to ion-exchange in solution caused a marked increase in the selectivity toward acetaldehyde at 300 °C. At variance, Fe ion-exchanged in the solid state resulted in a higher Brönsted acidity catalyst of higher selectivity to acetone. The solid state exchanged catalyst formed more coke at 400 °C. The higher zeolite acidity catalyzes the ethane propagation into the coke precursors. The extraordinary formation of ethane as a dominant transformation product (in the absence of H_2 gas supply) is explained mainly to the O-abstracting affinity of the Fe^{3+} ion. Methane may be formed as a result of decomposition reaction at high temperatures. Mössbauer and XRD were applied for characterizing different Fe species involved as active sites in the reaction. Coke deposited on the catalysts was measured by TGA. Other helpful information was obtained from BET of N_2-adsorption and FT–IR of NH_3-adsorption. Fair correlation between the active sites responsible for formation of the various products and the zeolite acidity is discussed along with a possible role for the surface area and pore structure in the reaction activity and selectivity.

Keywords: Ethanol reactions; Fe ion-exchanged mordenite; N_2- and NH_3-sorption; TGA; XRD; FT–IR; Mössbauer spectroscopy

1. Introduction

Isomorphous substitution of Fe into the zeolite framework has recently attracted increasing interest due to its unique and wide range applications in catalysis [1,2], e.g. the methanol oxidation [3], the oxidative dehydrogenation of propane [4] and the decomposition of *n*-butane [5] and of N_2O in the absence of any reducing agent [6]. The improved activity of Fe incorporated in the nano-space pores of the zeolites necessitates analysis of its coordination state and location in the zeolite structure. Diverse spectral techniques of FT–IR [7], EXAFS [8], ESR [9]and Mössbauer [10] were applied for probing the nature of the active sites associated with the modifier. The nano-space character of the zeolite pores determines to a large extent the range of fine particle metal ions upon the incorporation of Fe^{3+} ions in the zeolite [11,12]. Different routes of zeolite modification with Fe govern its dispersion in the catalyst. This should have varying consequences on the catalytic

E-mail address: mohmok2000@yahoo.com (M.M. Mohamed).

1381-1169/03/$ – see front matter © 2003 Elsevier Science B.V. All rights reserved.
doi:10.1016/S1381-1169(03)00093-1

properties, particularly the selectivity toward certain products [13].

Modification of zeolites with Fe by impregnation and ion-exchange led to formation of aggregated oxide clusters that are virtually inactive in a variety of reactions [14]. However, heat treatment increased the number and activity of such Fe species [15]. Selective oxidation of ethanol to more important chemicals has attracted industrial interest, particularly with the utilization of biomass as a chemical resource [16]. Molybdenum and vanadium oxide-based catalysts were tested for this reaction [17] for finding less expensive candidates than the commercial silver-based catalyst [18]. Superfine particles of Fe_2O_3, incorporated in the nano-space cavities of a zeolite like mordenite, have significantly enhanced the catalytic properties of the zeolite [15].

The aim of this study is to investigate the role of the tetrahedral and octahedral Fe in the ethanol transformation over Fe ion-exchanged mordenite, using XRD, BET and FT–IR of NH_3-adsorption along with the Fe-probe Mössbauer spectrometry. Possible role for varying methods of Fe incorporation in the mordenite structure in varying the transformation products of ethanol has been investigated by applying the ion-exchange with Fe in the solid as well as solution states.

2. Experimental

2.1. The catalyst preparation

The mordenite was of Conteka (Id. No. 122-90-003) brand of the SiO_2/Al_2O_3 ratio 5. The Na form was obtained from the H and NH_4 forms, using 0.1 M NaOH solution. Prior to exchanging the mordenite H^+, NH_4^+ and Na^+ cations into Fe^{3+}, the zeolite was thermally pretreated at the rate of $1.0^\circ\,min^{-1}$ where it was then kept at 300 °C for 3 h. Two methods were employed for preparing the Fe ion-exchanged mordenite catalysts. The Na-form mordenite was stirred in aqueous solutions of $FeSO_4{\cdot}7H_2O$ to give Fe loadings of 50, 100, 150 and 200%. The samples were labeled as 50, 100, 150 and 200 FeM, respectively. The 200% FeM zeolite sample was prepared on the basis of Fe^{2+} equals $2Na^+$ by adjusting the solution pH in the range of 5.5–7.0 [19]. Each loading was performed three times for accomplishing the required Fe content. The pure Fe-zeolites were dried at 110 °C for 5 h prior to calcination at 550 °C for 8 h. The Fe content in these zeolite catalysts was determined spectrophotometrically [20].

Ion-exchange in the solid state was performed for NH_4- or H-mordenite by mixing with $FeCl_3$ in the least amount of de-ionized water that would form a gel. The gels containing the stoichiometric amounts of Fe were dehydrated in an oven for 6 h at 110 °C and were eventually calcined in air at 550 °C for 8 h. The samples were designated as 100 $FeNH_4M$ and 100 FeHM, respectively.

2.2. Catalyst testing

Ethanol was reacted in a continuous flow fixed bed reactor containing 0.3 g catalyst crushed into 60–100 μm. Before catalysis in the temperature range of 200–400 °C, the catalyst was degassed under a flow of N_2 at 400 °C for 2 h. A stream of N_2 was passed through ethanol saturator at 7 °C for forming a gas mixture of 3 vol.% C_2H_5OH that should flow through the catalyst bed at a WHSV of $2.6\,h^{-1}$ from its top to the bottom. The reaction products were analyzed by on-line gas chromatography (Shimadzu 14A) using a stainless steel (2 m × 0.5 cm) column packed with 25% polyethylene glycolate absolute PEGA-supported Chromosorb P (250–350 μm) and a flame ionization detector.

2.3. Catalyst characterization

2.3.1. XRD analysis for the zeolite powder

The XRD powder patterns were recorded on a Philips (PW 1390) diffractometer, using Cu Kα radiation. The samples were measured in the 2θ range of 05–60° at 30 kV, 10 mA and a scanning rate of 2° in 2θ min^{-1}.

2.3.2. Mössbauer analysis for the nature of Fe incorporated in mordenite

Mössbauer spectra (MS) were recorded, using a constant acceleration spectrometer of 100 Ci ^{57}Co radioactive source in a Cr matrix. Iron metal was used for the calibration. Mössbauer spectra were analyzed, using a program based on the distribution of hyperfine magnetic field (HMF) and quadrupole splitting (QS).

2.3.3. FT–IR analyses for the pretreated zeolites and NH_3-sorption

The Fe-mordenite samples were pressed into self-supporting wafers of 20 mm diameter, mounted in an IR cell of CaF_2 windows and pretreated at pressured $<1.4 \times 10^{-2}$ Pa per 400°C. The zeolite acidity was measured for the pretreated samples after exposition to NH_3 gas at 150 °C for 30 min. followed by NH_3-desorption at 10^{-4} Torr per 200 °C for 15 min. The spectra were measured, using a 2 cm^{-1} resolution Jasco FT–IR 5300 spectrometer.

2.3.4. Surface area and pore structure analyses

Different surface characteristics of the catalysts investigated were studied using nitrogen adsorption isotherms conducted at −196 °C. The BET surface area (S_{BET}), total pore volume (V_P) and mean pore radius (r_H) were computed. Each sample was degassed by heating at 300 °C under reduced pressure of 10^{-5} Torr for 3 h.

2.3.5. TGA analysis of the coke deposits

TGA was performed for samples pre-used as catalysts in the ethanol transformation. Coke deposited on the zeolite catalyst was determined by burning under a stream of (30 cm^3 min^{-1}) dry air, using a Shimadzu 50A TGA in the range of 25–800 °C with a temperature rise of 10 °C min^{-1}.

3. Results and discussion

3.1. Mössbauer evaluation of active Fe sites

Activity and selectivity of the ethanol reactions were compared over the title catalysts in Tables 1 and 2, respectively. Methane and ethane are rather dominant products. Acetaldehyde and acetone are rather less dominant products. Diethyl ether is also detected as an inter-molecular dehydration product of ethanol. The reaction activity increases generally with increasing the reaction temperature. The Fe content was shown to affect the reaction activity that reaches maximum for the 100 FeM sample; the 150 and 200 FeM samples showed marked drop. Selectivity toward the ethane formation was a lot higher than for the other products. Methane was competing with acetaldehyde when raising the temperature to 400 °C. The amount of acetone was improved remarkably on improving the reaction activity whether by raising the reaction temperature or raising the Fe content. Diethyl ether forms in rather low percentages as a dehydration product at the external surface. The 100 FeHM sample showed exceptionally high (22%) amount of diethyl ether at 200 °C that drops with temperature to 4.4% at 300 °C and further to 2.2% at 400 °C. The 100 FeHM sample showed (Table 2) also high selectivity (33%) to acetone.

Table 1
Conversion (%), selectivities (%) and coke (%) of the ethanol transformation over the Fe-mordenite catalysts prepared by solution-state ion exchange

Catalyst	Temperature (°C)	Conversion (%)	Selectivity[a] (%)					
			CH_4	C_2H_6	$(C_2H_5)_2O$	CH_3CHO	$(CH_3)_2CO$	Coke
50 FeM	200	6.9	14.5	40.3	3.1	9.8	0.7	
	300	38.5	21.7	62.5	3.8	11.8	0.2	13.2
	400	54.2	19.0	59.3	2.6	7.5	11.6	
100 FeM	200	12.2	17.3	56.5	5.3	20.3	0.6	
	300	64.0	18.5	58.0	4.8	18.6	0.1	12.1
	400	68.0	19.3	61.7	2.6	7.0	9.4	
150 FeM	200	3.1	20.0	64.1	3.0	12.9		
	300	24.3	19.3	58.8	4.2	16.0	1.7	15.0
	400	35.3	15.4	50.2	3.3	11.0	20.1	
200 FeM	200	7.1	20.7	71.4	0.8	7.1		
	300	33.5	16.3	49.0	6.9	25.5	2.3	
	400	54.0	14.7	47.7	4.0	13.9	19.7	

[a] Selectivity was defined as $S = 100A_i/\Delta A$; with A_i: product area (wt.%); and ΔA: conversion area (wt.%).

Table 2
Conversion (%), selectivity (%) and coke (%) of the ethanol transformation over the Fe-mordenite catalysts prepared by solid-state ion exchange

Catalyst	Temperature (°C)	Conversion (%)	Selectivity[a] (%)					
			CH_4	C_2H_6	$(C_2H_5)_2O$	CH_3CHO	$(CH_3)_2CO$	Coke
100 $FeNH_4M$	100	0.72			21.0	79.0		
	200	75.90	21.5	66.7	2.6	9.2		20.1
	300	92.90	24.3	75.7				
	400	96.40	24.1	75.9				
100 FeHM	200	0.38	14.3	47.6	22.0	16.1		19.8
	300	7.90	15.0	48.5	4.4	17.0	15.1	
	400	23.60	12.2	40.7	2.2	11.9	33.0	

[a] Selectivity was defined as $S = 100A_i/\Delta A$; with A_i: product area (wt.%); and ΔA: conversion area (wt.%).

Dominance of the ethane product in the absence of H_2 may be due to oxygen abstraction from ethanol to ethane on account of finding appreciable amounts of Fe^{2+} species, as will be inspected in the 100 FeM sample using Mössbauer spectroscopy. This abstraction may be facilitated by extra-framework Fe species that exhibited similar role in many catalytic applications as found in FeMFI zeolite [21]. Deoxygenation of CH_3OH to CH_4 was similarly obtained over Fe/ZSM-5 catalyst [22] that produced high amounts of CH_4 as a function of Fe loadings. On the other hand, the IR spectral analysis of ethanol dehydrogenation and dehydration over metal oxides as MgO and Al_2O_3 have proven that surface ethoxide is a dominant intermediate [23,24]. On the basis of the above results, H_2 formation can occur when ethoxide was present on the surface in addition to acetaldehyde. It was known that when the inflow of ethanol stopped in the course of the reaction, the acetaldehyde formation decreased rapidly but H_2 formation lasted for a long time [23,24]. Concurrently, ethoxide can decompose into water and ether or ethylene in the course of dehydration. Thus, as tentative explanation the hydrogenation product, ethane, is formed as a result of the reaction of ethylene with H_2 produced from the dehydrogenation sequence with the assistance of surface hydroxyl groups.

Of particular importance, the formation of product with three carbon atoms, as acetone, from ethanol (two carbon atoms) can be explained if one consider the facile formation of Fe^{2+} components during the reaction; that will be elaborated in the coming section, which can react with acetic acid (expected product of acetaldehyde oxidation [25]) forming iron acetate that decomposes at high temperatures (400 °C) forming iron carbonate and acetone. This can be emphasized from noticing a decrease in selectivity of acetaldehyde in favor of acetone at high temperatures (400 °C) for all samples.

As another plausible explanation, Fe/zeolites can activate the methyl group [26] of acetic acid to form with another molecule of acetic, acetoacetic that finally underwent to decarboxylation forming acetone.

Varying the products selectivities over Fe-mordenite catalysts, either for those of solution- or solid-state ion exchange, suggest the participation of different active sites along with the acidity variation. More specifically, the active sites are more correspond to Fe species since carrying out a similar reaction, such as methanol transformation on mordenite zeolites, produced different products including alkenes and aromatics [27]. It is anticipated that iron-modified mordenite with relatively high iron contents proceed through either complete or incomplete ion exchange, those by their turn, would affect the final products distribution. The high Fe contents of the samples could also account for varying the products in these samples comparatively. Consequently, it is rather important utilizing Mössbauer spectroscopy on the catalysts before and after the reaction to reveal the active sites and their chemical quality.

Figs. 1 and 2 show the Mössbauer spectra (MS); collected at room temperature, of Fe-mordenite catalysts, namely 100 FeM, 100 FeHM and 100 $FeNH_4M$, after calcination (550 °C) and exposure to the reaction, respectively. The Mössbauer parameters and percentages

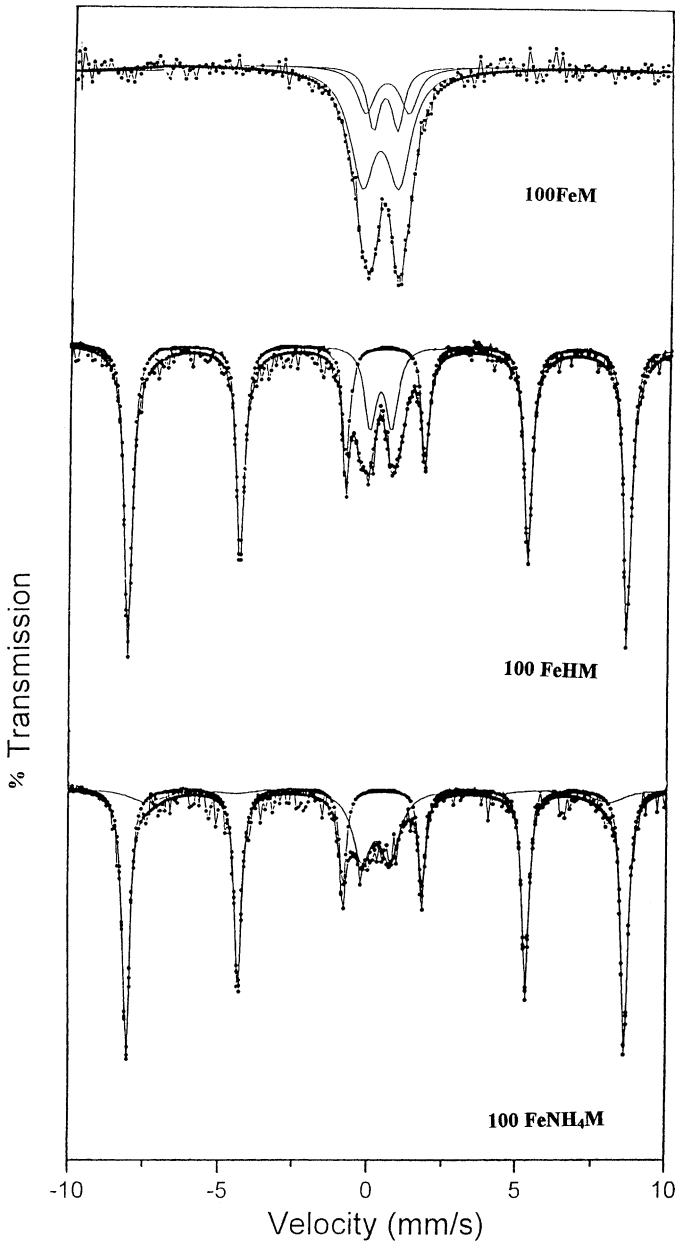

Fig. 1. Room temperature Mössbauer spectra of 100 FeM, 100 FeHM and 100 $FeNH_4M$ samples calcined at 550 °C.

of different Fe components are listed in Table 3. The spectrum of the 100 FeM catalyst (Fig. 1) shows three Fe^{3+} doublets: two of them are due to octahedral Fe^{3+}; [$Fe^{3+}(O)_1$ and $Fe^{3+}(O)_2$], where the third is due to tetrahedrally coordinated Fe^{3+} [$Fe^{3+}(T)$] that compromises a ratio equal 63.9% (Table 3). The existence of two doublets characterizing octahedral Fe^{3+}, with QS = 0.59 and 1.04 mm s^{-1}, could be a consequence of varying the crystallites size [28] or due to relaxation effects [29]. These species were corresponding to non-framework Fe^{3+} ($Fe^{3+}_{non\text{-}fram}$) that were probably occluded inside zeolite channels as nanoparticles

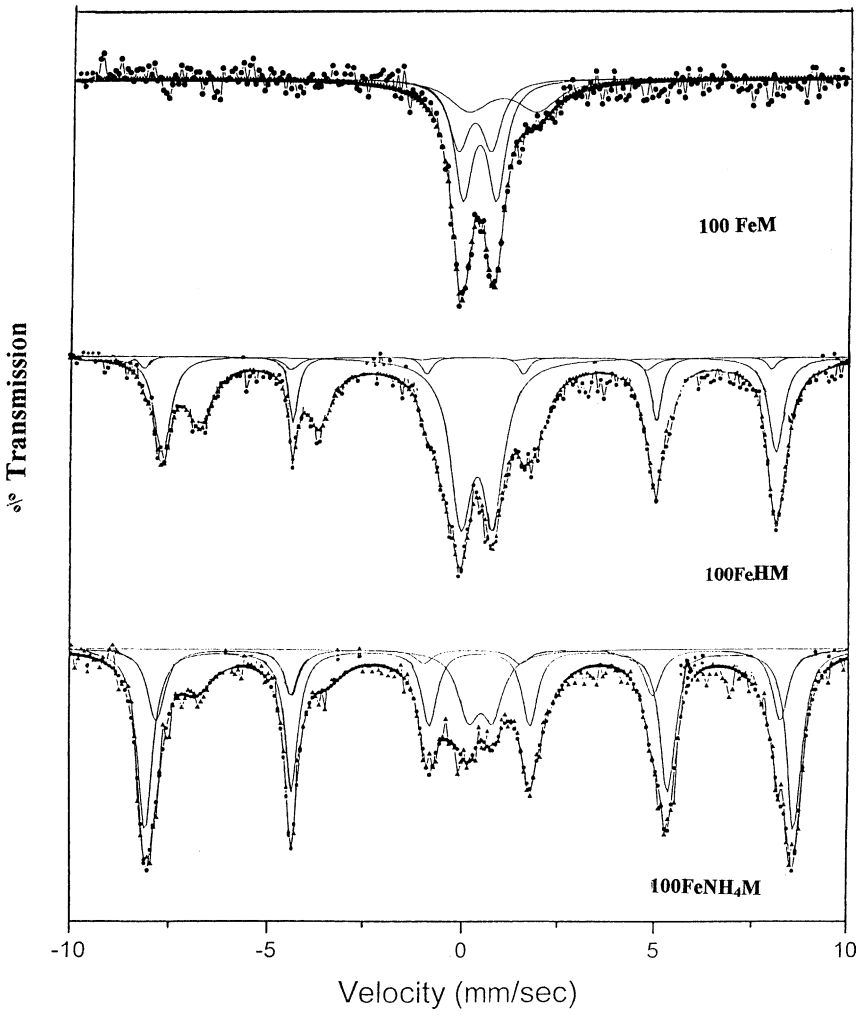

Fig. 2. Room temperature Mössbauer spectra of 100 FeM, 100 FeHM and 100 $FeNH_4M$ samples after performing the reaction.

or present on external surfaces. The presence of Fe^{3+} in tetrahedral symmetries (Fe^{3+}_{Td}) provided an evidence for their location in framework T sites substituting for Al. After performing the reaction on the sample (Fig. 2), it shows three overlapping paramagnetic doublets with distinct differences from those in Fig. 1. The first important feature is the increase in Fe^{3+} occupied octahedral sites (45%) forming one phase of uniform particles size, and diminishing that of Fe^{3+} occupied tetrahedral (28%, Table 3) sites. The second important feature is the existence of Fe^{2+} component (27%). This could be explained as resulting from reduction [30]. Since, the reduction is characteristic also for extra-framework ions, this component can probably attributed to the counterpart extra-framework ions in Fe-silicate structures, i.e. proportional to $(Si/Fe)^{2-}$ [2,31]. Provoking the formation of Fe^{2+} components could also be connected to ethanol due to its reducing action.

From what has been presented using MS for the 100 FeM sample, which showed the highest ethanol conversion over all samples (Table 1), two predominant species can be revealed: first is Fe^{3+}_{Td} that underwent to a considerable removal from the framework during the reaction. Second is extra-framework Fe species that participates by two different phases (hetero-phase)

Table 3
Mössbauer parameters of the spectra shown in Figs. 1 and 2

Sample	$Fe^{3+}(O)_1$			$Fe^{3+}(O)_2$			$Fe^{3+}(T)$			α-Fe_2O_3			
	IS ($mm\,s^{-1}$)	QS ($mm\,s^{-1}$)	Area (%)	IS ($mm\,s^{-1}$)	QS ($mm\,s^{-1}$)	Area (%)	IS ($mm\,s^{-1}$)	QS ($mm\,s^{-1}$)	Area (%)	IS ($mm\,s^{-1}$)	QS ($mm\,s^{-1}$)	H (kOe)	Area (%)
100 FeM													
Fresh	0.4	0.59	17	0.45	1.04	19.1	0.27	0.87	63.9				
Used	0.42	0.9	45	1.05	1.84	27	0.29	0.88	28				
100 FeHM													
Fresh							0.29	1.29	11.4	0.37	−0.27	516	76.8
							0.3	0.72	11.8				
Used							0.3	1.3	11	0.37	−0.21	516	61
										0.27	−0.28	482	5
100 $FeNH_4M$													
Fresh							0.29	0.93	21.3	0.37	−0.22	516	67.4
										0.27	0.28	478	11.3
Used	0.3	1.3	11				0.3	0.7	13	0.37	−0.21	516	59
										0.36	−0.16	510	11
										0.27	0.23	485	6

Note: IS, isomer shift; QS, electric quadrupole splitting; H, mean hyperfine field. Highlighted numbers are correspond to Ferrous octahedral component. Fresh and used mean before and after performing the reaction, respectively.

before the reaction and dislodged as one phase after the reaction. This implies that portions of extra-framework Fe species may take part in the reaction as highly dispersed α-Fe_2O_3 particles. The probability of accommodating Fe in mordenite framework, as highly dispersed oxide, as devoted before for Y zeolite [32], is verified by the lack of magnetic splitting in the spectra of 100 FeM either before or after performing the reaction, i.e. small magnetic particles may exhibit paramagnetic resonance spectra provided their characteristic size exceeds a threshold value [2]. As a further confirmation, performing the Mössbauer measurements at low temperatures as 20 K for the 150 FeM sample [10] showed the disappearance of both $Fe^{3+}(O)$ phases and the appearance of a magnetic six-line phase, which has the parameters of α-Fe_2O_3 [33]. These results indicated that both $Fe^{3+}(O)_1$ and $Fe^{3+}(O)_2$ represent super-paramagnetic α-Fe_2O_3 in different particles size. On the other hand, decreasing the conversion for the rest of the samples (Table 1) when compared with that of 100 FeM can be due to either decreasing Fe^{3+}_{Td} species or increasing the Fe^{3+}_{Oh} ones or both [10]. This has been evidenced from the results of the samples relative area that showed a marked decrease in Fe^{3+} occupied tetrahedral symmetry upon increasing the Fe loading, e.g. 73.6% for 50 FeM versus 41% for 200 FeM. Inspection the above results and correlating it with the product distribution data obtained from ethanol conversion over various catalysts summarized in Table 1, revealed the followings. The increased selectivity to acetone at 400 °C over 200 FeM, at relatively high conversions, imposes the importance of extra-framework Fe species as active sites for acetone formation. This emphasizes the suggested way of acetone formation; of iron acetate, because extra-framework Fe^{3+} species are more eligible to produce Fe^{2+} components during the reaction. The comparatively low temperature activity towards acetaldehyde at 300 °C, on one hand, and its decrease at high temperature, on the other hand, can be due to its condensation (as Aldol) and thus heavier products are formed that can be adsorbed at the surface. One would expect that the small size α-Fe_2O_3 encapsulated inside mordenite channels would reduce the shape selective effects and should, consequently, increase the activity towards oxidation products. The dispersion issue will be elaborated clearly in the coming section using XRD results.

Inspecting the MS of the solid-state ion exchange of $FeCl_3$ (at 100% loading) with either HM or NH_4M before and after the reaction revealed the followings.

The most noticeable feature is the restoration of tetrahedral Fe^{3+} components for the sample derived from HM while a marked decrease was depicted for the one derived from NH_4M, indicating an appreciable contribution of Fe^{3+}(T) components in the reaction. On the other hand, both of the samples were fitted with three overlapping sextets, after the reaction, representing well and poorly crystallized α-Fe_2O_3 (Table 3). The decrease of the values of HMF of the second and third broad α-Fe_2O_3 phases, as for example, 498 and 482 for 100 FeHM and 485 for 100 $FeNH_4M$ indicated that these phases may principally be due to the decreased particles size [34]. In the light of detailed Mössbauer analyses some understanding on the nature of active catalytic sites can be revealed. Mössbauer data substantiate the importance of the hematite phase as active sites for the reaction. The marked increase in the conversion of ethanol transformation over 100 $FeNH_4M$ if compared with 100 FeHM at all reaction temperatures could be due to finely dispersed α-Fe_2O_3 particles and to the increased surface area of 100 $FeNH_4M$ over that of 100 FeHM, as will be discussed later. In the light of last mentioned characteristics, the former sample exhibited higher selectivity for methane and ethane than the rest of the samples. The highest selectivity to ethane and methane at 300 and 400 °C occurs over 100$FeNH_4M$ at high conversions (92 and 96%, respectively), however, no product of ether or acetaldehyde can be detected. This may be a consequence of either changing the Fe species (Table 3), specifically those of non-framework, or subtle acidity change that could be confined of Brönsted sites, formed after ammonia decomposition.

The calculated amount of coke that was obtained using TGA as the difference in the loss in weight for the samples before and after the reaction showed different variations (Tables 1 and 2). The relatively high amounts of coke produced for 100 FeHM and 100 $FeNH_4M$ samples are indicative of the strong hydrocarbon adsorption on their surfaces. As can be seen the product distribution obtained over these samples was different from those over the rest of the samples (Table 1). In this context, the 100 $FeNH_4M$ catalyst did not show any condensation (diethyl ether) and dehydrogenation (acetaldehyde) products in the temperature range of 300–400 °C. On the other hand, the 150 FeM and 200 FeM samples showed high selectivities for CH_4 and C_2H_6 (Table 1) in addition to appreciable amounts of condensation and dehydrogenation products and acetone. This possibly due to lowering the acidity of Fe-mordenite samples derived from NaM rather than those obtained from HM or NH_4M samples.

3.2. Surface characteristics and acidity of different investigated catalysts

The different surface characteristics namely S_{BET}, V_p and r_H were determined for each catalyst sample. The results obtained are given in Table 4. It can be seen from this Table that S_{BET} of HM increases by treating with different proportions of $FeSO_4$ reaching a maximum limit for the 100 FeM sample, an increase of about 66%. An opposite effect was manifested upon treating the HM sample with 100% $FeCl_3$ using the mechanical mixing procedure, a decrease of about

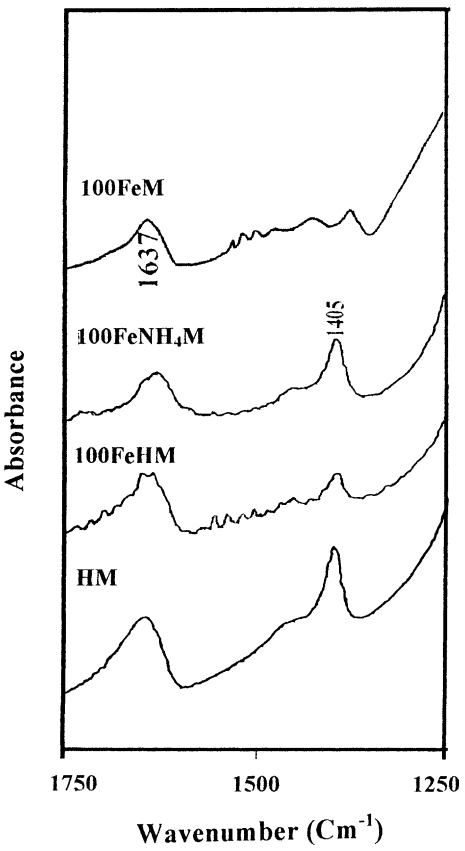

Fig. 3. IR spectra of chemisorbed ammonia on HM, 100 FeM, 100 FeHM and 100 $FeNH_4M$ samples.

Table 4
Surface characteristics and X-ray data of the title catalyst samples

Sample	S_{BET} ($m^2\,g^{-1}$)	V_P ($ml\,g^{-1}$)	r_H (Å)	Crystallinity (%)
HM	340	0.63	53.4	100.0
50 FeM	485	0.59	30.1	82
100 FeM	564	0.56	24.5	77
150 FeM	465	0.60	32.9	83
200 FeM	495	0.53	26.8	80
100 FeHM	276	0.45	40.5	67
100 $FeNH_4M$	566	0.54	23.7	67

Where S_{BET} is the BET surface area, r_H is the value of the average pore radius and V_P is the total pore volume. The crystallinity was obtained from sum of the intensities of some diffraction lines. The original HM was taken as reference of 100% crystallinity.

19%. These findings clarify the role of method of preparation in modifying the specific surface area of the treated zeolite. On the other hand, the total pore volume of the HM suffers a slight decrease by treating with $FeSO_4$ or $FeCl_3$. The decrease in the V_P value was, however, more pronounced in the case of HM mechanically treated with $FeCl_3$ (100 FeHM). The observed net increase in the S_{BET} of 100% $FeCl_3$ treated NH_4M (100 $FeNH_4M$) could be attributed to the effective pore narrowing process. In fact the r_H value decreases from 53.4 to 23.7 Å. This can be facilitated by departure of ammonia during the mechanical mixing of $FeCl_3$ with NH_4M. In fact it has been reported [35] that the texture of NH_4M exposed narrower pores than that of HM where those of wide pores of the former are preferably filled leaving behind the narrow ones those responsible for enhancing the area of modified NH_4M sample comparatively. On the other hand, the texture of HM was mainly consisted of wider pores than that revealed in the NH_4M sample.

The XRD results of the samples, prepared by liquid-state ion exchange, revealed minor changes in the crystallinity albeit the over exchange that reached

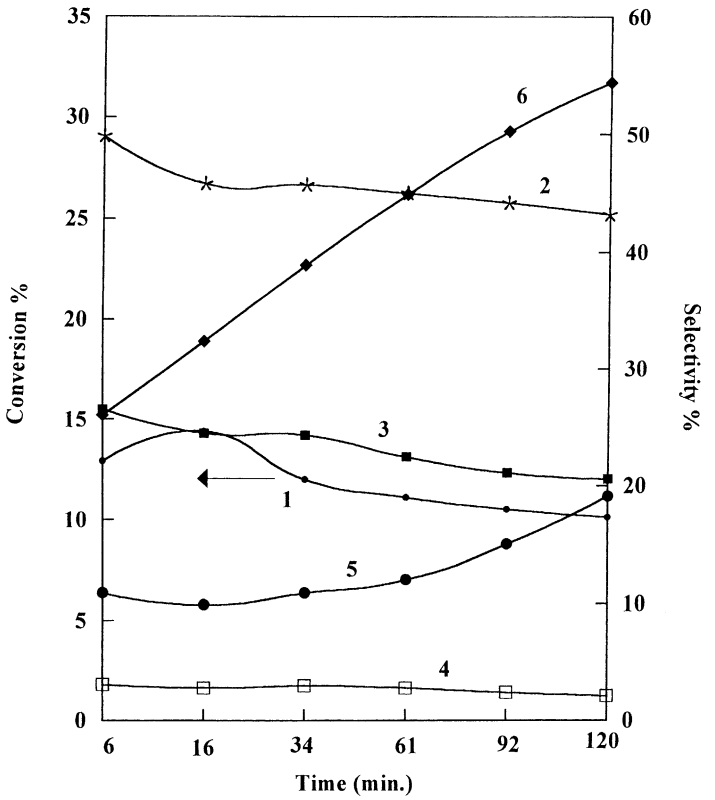

Fig. 4. Change in ethanol conversion (curve 1) and selectivity to methane (curve 2), ethane (curve 3), ether (curve 4), acetaldehyde (curve 5) and acetone (curve 6) over 100 FeHM at reaction temperature 350 °C.

200%. This suggests that the structure of the zeolite has not been much affected following the preparation. It is worth mentioning to report the absence of any diffraction lines of α-Fe_2O_3 phase. So, one might suggest the presence of such phase in a finely divided state, i.e. having particles size below the detection limit of XRD (below 20 Å). On the other hand, the XRD measurements of the samples derived from solid-state ion exchange showed new diffraction lines at $2\theta = 33.13$, 49.85 and 54.11° that were ascribed to the most intensive lines of hematite phase. This indeed indicates that α-Fe_2O_3 is formed in the outermost surface layer of mordenite channels.

Ammonia was applied as a smaller probe molecule than pyridine to characterize the surface acidity of various samples. FT–IR of ammonia adsorbed on some representative samples; namely 100 FeM, 100 FeHM and 100 $FeNH_4M$ in comparison with HM, are shown in Fig. 3. The HM spectrum shows bands at 1647 and 1405 (1445) cm^{-1}, which are characteristic of either strongly bonded ammonia or adsorbed water and asymmetric deformation mode of ammonium ion (δ_{as} NH_4^+) [36], respectively. The spectrum of adsorbed ammonia on 100 FeM shows a remarkable decrease in intensities of all bands.

On the other hand, the 100 FeHM sample showed bands at 1405, 1457 and 1637 cm^{-1}. It can be seen that the 100 FeHM sample possesses higher acidity than the 100 FeM one. For the 100 $FeNH_4M$ sample, similar bands as those found on 100 FeHM (1405, 1457 and 1630 cm^{-1}) were detected. A marked increase in intensity of the 1405 cm^{-1} band appeared on the former than that on the latter. The shift of the band at 1647 cm^{-1} to lower wavenumbers; (1637 cm^{-1} in FeM and 1630 cm^{-1} in FeHM and $FeNH_4M$), could be an indication of finding some Lewis acidity, i.e. NH_3 coordinated to Fe^{3+}. This result has been evidenced by the work of Liepold et al. [37] during the investiga-

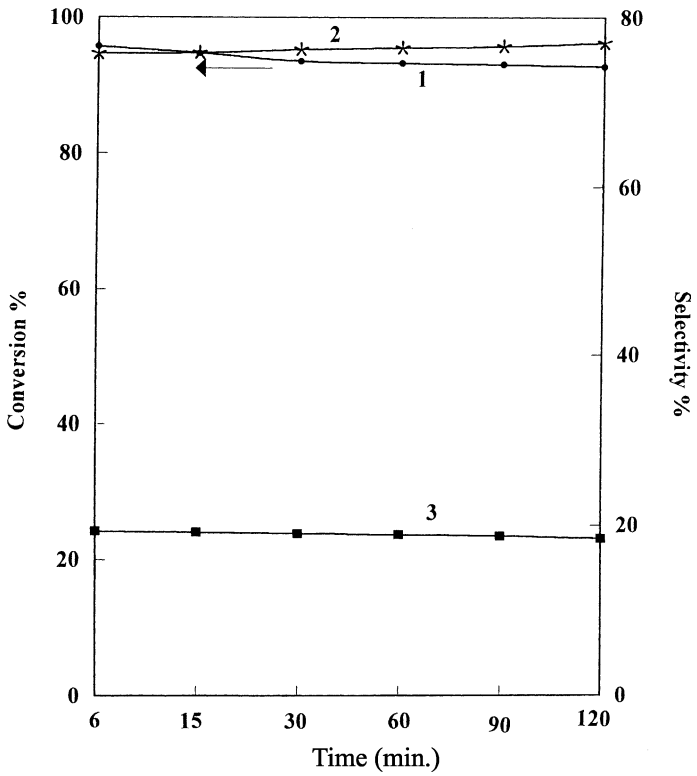

Fig. 5. Change in ethanol conversion (curve 1) and selectivity to methane (curve 2), ethane (curve 3), ether (curve 4), acetaldehyde (curve 5) and to acetone (curve 6) over 100 $FeNH_4M$ at reaction temperature 350 °C.

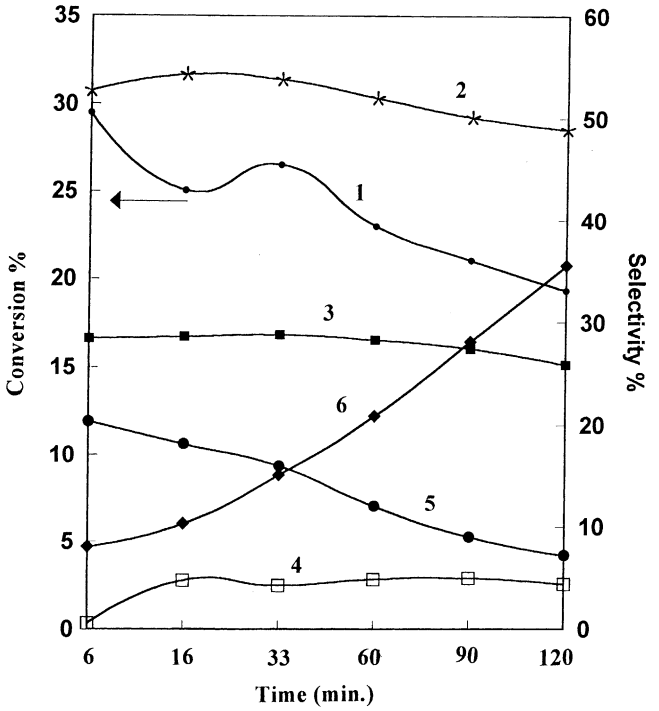

Fig. 6. Change in ethanol conversion (curve 1) and selectivity to methane (curve 2), ethane (curve 3), ether (curve 4), acetaldehyde (curve 5) and acetone (curve 6) over 150 FeHM at reaction temperature 350 °C.

tion of acid sites of aluminosilicate MCM-41 by ammonia adsorption. They noticed a band at 1625 cm^{-1} that has been assigned to Lewis acid sites. From what has been presented, it has been proved that the density of acid sites especially Brönsted ones was markedly decreased; in solution-state ion exchanged samples, with increasing the Fe contents, due to the replacement of Al(OH)Si by Fe(OH)Si of more covalent character. However, with regard to 100 $FeNH_4M$ a rather strong band at 1405 cm^{-1}, assigned to protonated ammonia molecules being adsorbed at Brönsted acidic sites is detected besides a band at 1630 cm^{-1} represents strong coordinative bonds of ammonia, interacting with Lewis acidic sites. This increase in the number of acidic sites of 100 $FeNH_4M$ over those of 100 FeM and 100 FeHM was in very good agreement with the results of conversion (Tables 1and 2). Judged by the comparison of the results obtained over 100 FeHM and 100 $FeNH_4M$, the presence of a definite number of acidic sites seems to promote the selective oxidation products of ethanol as for 100 FeHM that provides active iron sites as well as moderate acidic sites capable of producing appreciable selectivity to acetone.

3.3. Catalysts selectivities and durabilities

Figs. 4–7 show the change in ethanol conversion and selectivity, to various products, versus time-on-stream over 100 FeHM, 100 $FeNH_4M$, 150 FeM and 200 FeM catalysts, respectively, at 350 °C. The results obtained for the transformation of ethanol to ethane are consistent with the higher acidity that was observed for the 100 $FeNH_4M$ catalyst. Furthermore, the high selectivity of ethane could be due to rapid conversion of alkenes on strong acid sites [38] and thus favoring hydride transfer. The formation of ethane as the main reaction product can be rationalized to the recognized high electron affinity of Fe^{3+} ions. On the other hand, the active sites that possess moderate interaction with both reactants and products, as 100 FeHM, generates high selectivities to acetone and acetaldehyde but the conversion is among the lowest. This sample

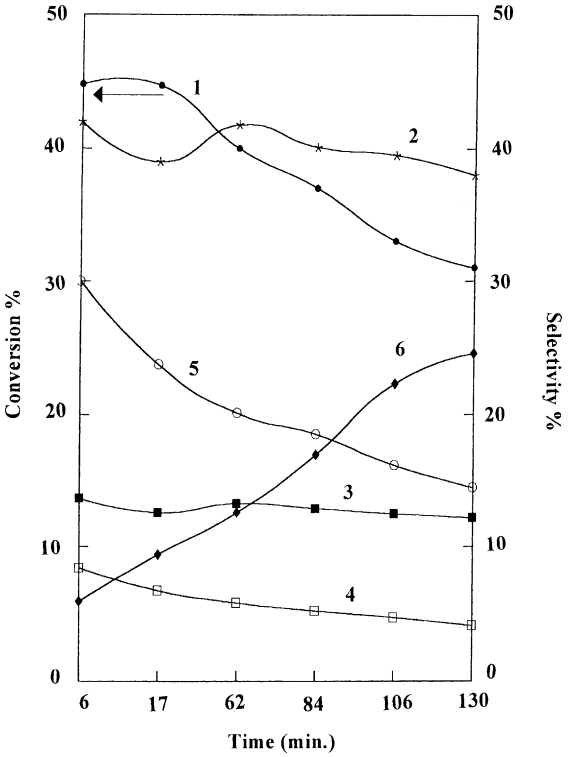

Fig. 7. Change in ethanol conversion (curve 1) and selectivity to methane (curve 2), ethane (curve 3), ether (curve 4), acetaldehyde (curve 5) and acetone (curve 6) over 200 FeM at reaction temperature 350 °C.

also showed a decrease in selectivities to ethane and methane with time. The selectivity to diethyl ether that appears to be catalyzed by Lewis acid sites, as indicated by others [39], showed a decrease on 100 FeHM compared with the other samples. This may due to the deposition of high amounts of carbon in the case of 100 FeHM motivating the blockage of Lewis sites.

Lowering the acidity as well as changing the Fe components for 150 and 200 FeM samples affect the conversion that drops to values comprise 20–25% at around 120–130 min. As a result the selectivity to acetone was increased with time. The maximum value was 36% for the 150 FeM sample, where the amounts of other products decreased (acetaldehyde and ethane) or remained practically constant (methane) with time. This indicates that acetone formation is somehow dependent on rather low amounts of Brönsted acidic sites; besides the high oxidizing ability, that are profitable for ascetic acid formation during the oxidation of acetaldehyde and then proceed to from acetone, as mentioned before. The 100 FeHM sample showed high durability and selectivity based on the presence of α-Fe_2O_3 species and to the moderate acidity of their sites. The distribution of the products remained practically unchanged with time-on-stream for 100 $FeNH_4M$ and 100 FeHM samples, where they relatively changed for 150 and 200 FeM samples. This could be related to the continuous changes of Fe species in these samples during the reaction. For the duration of the runs, approximately 120 min, no marked deactivation was observed for any of the samples.

4. Conclusions

From the experimental results obtained over Fe exchanged mordenite zeolites, either prepared by liquid- or solid-state ion exchange, the following conclusions can be drawn.

- The conversion values obtained for ethanol transformation were markedly higher with 100 $FeNH_4M$ than the rest of the catalysts, in accordance with the higher acidity of its sites and larger value of its BET surface area. The selectivity towards ether (200 °C), acetaldehyde (300 °C) and acetone (400 °C) was enhanced over 100 FeHM due to moderate acidity and to the independence of the products selectivity on either the surface area or the particles size of α-Fe_2O_3, those affected mainly the values of conversion. In contrary, the conversion values of the former samples were much higher than those of the latter. This let us conclude that the selectivity behavior are more correspond to acid sites, where the conversion can be considered as a function of different parameters including the dispersion of different Fe species that positively affected the surface area values.
- It seems that the conversion of ethanol can be accelerated by various Fe species specifically those in framework positions and those exhibiting finally dispersed α-Fe_2O_3 species. The latter species were markedly improved the conversion values over the former ones.

Acknowledgements

The author thanks Professor R. Gabr from Assiut University for allowing to carrying out the activity measurements in his laboratories.

References

[1] L. Brabec, M. Jeschke, R. Klik, J. Novakova, L. Kubelkova, J. Meusinger, Appl. Catal. 170 (1998) 105.
[2] P. Fejes, J.B. Nagy, K. Lazar, J. Halasz, Appl. Catal Part A: Gen. 190 (2000) 117.
[3] G.J. Kim, W.S. Ahn, Appl. Catal. 71 (1991) 55.
[4] M.A. Uddin, T. Komatsu, T. Yashima, J. Catal. 150 (1994) 439.
[5] M.A. Uddin, T. Komatsu, T. Yashima, Chem. Lett. (1993) 1037.
[6] M. Rauscher, K. Kesore, R. Monning, W. Schwieger, A. Tibler, T. Turek, Appl. Catal. Part A: Gen. 184 (1999) 249.
[7] A. Zecchina, F. Geobaldo, C. Lamberti, S. Bordijo, G.T. Palomino, C.O. Arean, Catal. Lett. 42 (1996) 25.
[8] N. Matsubayashi, H. Shimada, M. Imamura, T. Sato, K. Okabe, Y. Yoshimura, A. Nishijima, Catal. Today 29 (1996) 273.
[9] B. Wichterlova, S. Beran, S. Bednarova, K. Nedomova, L. Dudikova, P. Jiru, Stud. Surf. Sci. Catal. 37 (1988) 199.
[10] M.M. Mohamed, N.S. Gomaa, M. El-Moselhy, J. Colloid Interface Sci., in press.
[11] M.M. Mohamed, T.M. Salama, R. Ohnishi, M. Ichikawa, Langmuir 17 (2001) 5678.
[12] M.M. Mohamed, M. Ichikawa, J. Mol. Catal., submitted for publication.
[13] K. Hashimoto, N. Toukai, Appl. Catal. Part A: Gen. 180 (1999) 367.
[14] B. Coq, D. Tachon, F. Figueras, G. Mabilon, M. Pringent, Appl. Catal. B 6 (1995) 271.
[15] P. Fejes, J.B. Nagy, J. Halasz, A. Oszko, Appl. Catal Part A: Gen. 175 (1998) 89.
[16] B.O. Palsson, S. Fathi-Afshar, D.F. Rudd, E.N. Lightfoot, Science 213 (1981) 513.
[17] J.E. Lgosdon, Kirk-Othmer Encyclopedia of Chemical Technology, 4th ed., vol. 9, Wiley, New York, 1994, p. 812.
[18] H.H. Kung, Transition Metal Oxides-Surface Chemistry and Catalysis Stud. Surf. Sci. Catal., vol. 45, Elsevier, Amsterdam, 1989, p. 200.
[19] W.K. Hall, X. Feng, J. Dumesic, R. Watwe, Catal. Lett. 52 (1998) 13.
[20] M.T.M. Zaki, A.Y. El Sayed, Fresenius Z. Anal. Chim. 334 (1989) 335.
[21] J. Perez-Ramirez, F. Kaptein, G. Mul, J.A. Moulijn, Catal. Commun. 3 (2002) 19.
[22] A. Mahay, G. Lemay, A. Adnot, I.M. Szoghy, S. Kaliaguine, J. Catal. 103 (1987) 480.
[23] N. Takezawa, C. Hanamaki, H. Kobayshi, J. Catal. 38 (1975) 101.
[24] N. Takezawa, H. Kobayshi, J. Catal. 28 (1973) 335.
[25] K. Nowinska, M. Sopa, D. Szuba, Catal. Lett. 39 (1996) 275.
[26] M.B. Sayed, J. Chem. Soc., Faraday Trans. I 83 (1987) 1771; N.M. Marinov, Int. J. Chem. Kinet. 31 (1999) 183.
[27] A.J. Marchi, G.F. Firoment, Appl. Catal. Part A: Gen. 94 (1993) 91.
[28] L. Haggstrorn, H. Annerten, T. Ericsson, R. Wappling, W. Karner, S. Bjarman, Hyperfine Intract. 201 (1978) 5.
[29] M. Blume, Phys. Rev. Lett. 14 (1965) 96.
[30] K. Lazar, G. Borbely, H.K. Beyer, H.G. Karge, J. Chem. Soc., Faraday Trans. 90 (1994) 1329.
[31] G.P. Huffman, B. Ganguly, J. Zhao, K.R.P.M. Rao, N. Shah, Z. Feng, F.E. Huggins, M.M. Taghili, F. Lu, L. Wenders, V.R. Pradhan, J.W. Tierney, M.S. Seehra, M.M. Ibrahim, J. Shabtai, E.M. Eyring, Energy Fuels 7 (1993) 285.
[32] Y. Okamoto, H. Kihuta, Y. Ohto, S. Nasu, O. Terasaki, Stud. Surf. Sci. Catal. 105 (1997) 2051.
[33] J.L. Dormann, Rev. Phys. Appl. 16 (1981) 275.
[34] B.A. Morrow, I.A. Cody, J. Catal. 45 (1976) 51.
[35] M. El Moseley, Master Thesis, Al-Azhar University, 2002.
[36] M.D. Amirdis, F. Puglisi, J.A. Damesic, W.S. Millinaan, N. Yu, J. Topsoe, J. Catal. 142 (1993) 571.
[37] A. Liepold, K. Roos, W. Reschetilowski, R. Schmidt, M. Stocker, A. Philippou, N.W. Anderson, A.P. Esculcas, J. Rocha, In: S.K Ihm, Y. S. Uh. (Eds.), Stud. Surf. Catal. 105 (1997) 423.
[38] A.J. Marchi, G.F. Froment, Appl. Catal. Part A: Gen. 94 (1993) 91.
[39] M.B. Sayed, R.P. Cooney, Aust. J. Chem. 35 (1982) 2483.